Complementary Sets of Shutter Sequences for Motion Deblurring

Hae-Gon Jeon[1] Joon-Young Lee[1] Yudeog Han[2] Seon Joo Kim[3] In So Kweon[1]
[1] Robotics and Computer Vision Lab., KAIST [2] Agency for Defense Development [3] Yonsei Univerisity
hgjeon@rcv.kaist.ac.kr jylee@rcv.kaist.ac.kr ydhan@add.re.kr seonjookim@yonsei.ac.kr iskweon@kaist.ac.kr

Abstract

In this paper, we present a novel multi-image motion deblurring method utilizing the coded exposure technique. The key idea of our work is to capture video frames with a set of complementary fluttering patterns to preserve spatial frequency details. We introduce an algorithm for generating a complementary set of binary sequences based on the modern communication theory and implement the coded exposure video system with an off-the-shelf machine vision camera. The effectiveness of our method is demonstrated on various challenging examples with quantitative and qualitative comparisons to other computational image capturing methods used for image deblurring.

1. Introduction

Image deblurring is a challenging task that is inherently an ill-posed problem due to the loss of high frequency information during the imaging process. In the past decade, there have been significant developments in the image deblurring research that improve the performance over the traditional deblurring solutions such as Richardson-Lucy [29, 23] and Wiener filter [42].

One research direction that has gained interest is to use multiple blurred images for deblurring, which shows better performance over the single image deblurring methods in general due to the complementary information provided. Yuan *et al*. used a blurred/noise image pairs to estimate the blur kernel [43], Cai *et al*. proposed to use multiple severly motion blurred images [4], and Chen *et al*. performed an iterative blur kernel estimation and a dual image deblurring [6]. Cho *et al*. [7] presented a video deblurring approach that uses sharp regions in a frame to restore blurry regions of the same content in nearby frames. In [32, 33], motion blur in a video is reduced by increasing the framerate for temporal super-resolution.

Another development in the image deblurring research is to modify the way images are captured to make the deblurring problem more feasible. In [21, 20, 28], videos are captured by modulating each pixel independently by binary patterns, which enables the recovery of high temporal resolution. On the other hand, this paper is particularly related to the works that employ imaging systems that control the exposures for the whole image, not on the pixel level, during image captures. In [27], Raskar *et al*. presented the coded exposure photography that flutters the camera's shutter open and closed in a special manner within the exposure time in order to preserve the spatial frequency details, thereby enabling the deconvolution problem to become well-posed (Fig. 1(a)). Jeon *et al*. [14] improved deconvolution performance by computing optimized fluttering patterns.

Instead of the fluttering shutter within a single exposure, Agrawal *et al*. [2] proposed a varying exposure video framework which varies the exposure time of successive frames (Fig. 1(b)). The main idea is to image the same object with varying PSFs (Point Spread Functions) by varying the exposures so that the nulls in the frequency component of one frame can be filled by other frames, making the deblurring problem well-posed. Holloway *et al*. [12] applied the concept of coded exposure into a video camera. This approach captures a series of coded exposure images with different fluttering patterns in successive frames and perform temporal resolution upsampling via compressed sensing. As mentioned in [12], this approach cannot handle scenes without the spatio-temporal continuity and requires many observations for estimating an object motion.

In this paper, we propose a coded exposure video scheme which combines the benefits of the coded exposure imaging [27, 14] and the varying exposure video [2]. Rather than varying the exposures between the frames, we capture a video under a fixed exposure time and apply the coded exposure on each frame (Fig. 1(c)). To minimize the frequency information loss during the image capture, we introduce a method for generating a complementary set of fluttering patterns that compensate for the losses in successive frames. By using the complementary sets of fluttering patterns, we can generate various exposure time sequences for a flexible frame rate capture and achieve higher quality deblurring results with improved SNR compared to the previous methods. In addition, we show our framework can be applied to other application such as the privacy protection for video surveillance by adding intentional blur [19].

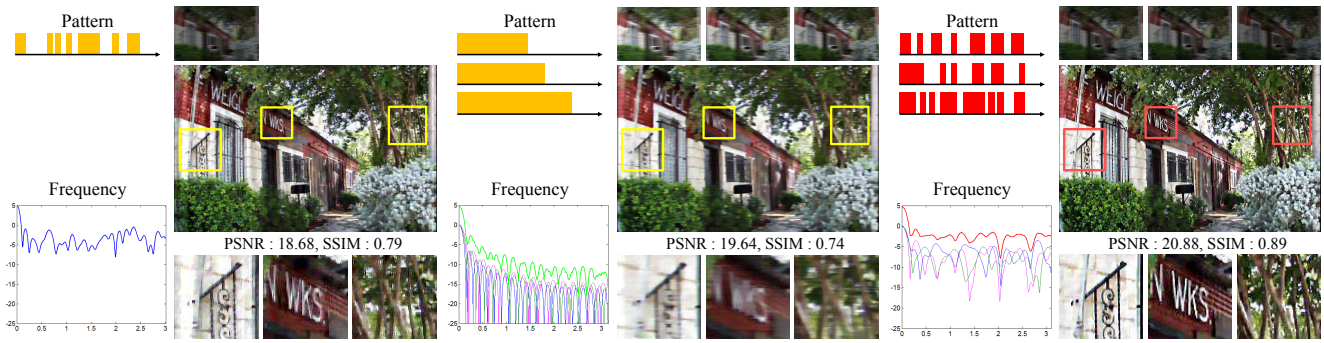

(a) (b) (c)

Figure 1. Comparisons of different computational imaging techniques for image deblurring. (a) Coded exposure imaging [27]. (b) Varying exposure video [2]. (c) Proposed coded exposure video.

2. Complementary Set of Sequences and Coded Exposure

The key idea of this paper is to capture video frames with a set of fluttering patterns that compensate frequency losses in each frame, so that the captured images preserve spatial frequencies. To generate such fluttering patterns, we introduce a *complementary set* of binary sequences [38], which is widely used in many engineering applications such as the multiple-input multiple-output (MIMO) radar and the code division multiple access (CDMA) technique [35]. In this section, we theoretically show the advantage of the coded exposure video with the complementary set of fluttering patterns over the coded exposure imaging [27, 14] and the varying exposure video [2].

2.1. Coded Exposure Imaging vs. Coded Exposure Video

In [27], it has been shown that a fluttering pattern with a flat spectrum improves the quality of the deblurring in the coded exposure imaging. To measure the flatness, they use the sum of an autocovariance function of a fluttering pattern. It is also shown in [14] that an autocorrelation function of a binary sequence can be approximated by an autocovariance function. With a binary sequence $U = [u_1, \cdots, u_n]$ of length n, the relationship between the autocorrelation and the modulated transfer function (MTF : a magnitude of frequency response of binary sequence) via the Fourier transform of the sequence is derived as ([13])

$$\sum_{k=1}^{n-1} \Psi_k^2 = \frac{1}{2} \int_0^1 \left[|\mathcal{F}(U)|^2 - n \right]^2 d\theta, \tag{1}$$

where $\mathcal{F}(U)$ represents the Fourier transform of the sequence U. Ψ_k denotes k^{th} element of the autocorrelation function Ψ of the sequence, which is defined as

$$\Psi_k = \sum_{j=1}^{n-k} u_j u_{j+k}. \tag{2}$$

In [14], it is shown that a smaller value of Eq. (1) reflects higher merit factor, which in turn results in better deblurring performance. Ukil proves in [39] that the minimum value of Eq. (1) is bounded by $n/2$.

In our coded exposure video framework, a complementary set is defined as a set of binary sequences where the sum of autocorrelation functions of the sequences in the set is zero. If we have a complementary set $\mathbf{\Delta}$ consisting of $p(\geq 2)$ sequences $\{U_1, \cdots, U_p\}$ of length n, the relationship is denoted as

$$\sum_{i=1}^{p} \Psi_k^i = 0 \quad \text{s.t.} \quad k \neq 0, \tag{3}$$

where Ψ_k^i denotes k^{th} element of the autocorrelation function Ψ of the i^{th} sequence in $\mathbf{\Delta}$.

It is shown in [34] that a complementary set $\mathbf{\Delta}$ is computed by minimizing

$$\sum_{k=1}^{n-1} |\sum_{i=1}^{p} \Psi_k^i|^2 = \frac{1}{2} \int_0^1 \left[\sum_{i=1}^{p} |\mathcal{F}(U_i)|^2 - pn \right]^2 d\theta. \tag{4}$$

In the optimal case, the minimum value of Eq. (4) becomes zero from Eq. (3). This means that the joint spectrum of a complementary set has flatter spectrum than that of a single binary sequence (coded exposure imaging) since Eq. (1) is bounded to $n/2$ for a single binary sequence as mentioned above. We estimate a spectral gain of one example complementary set of sequences using a numerical measure, proposed by Tendero *et al.* [37], and the gain of the sequence set is 0.85 while the gain of an optimal snapshot of a single coded pattern is 0.56.

2.2. Performance Invariance to Object Velocity

When the object moves over a range of n pixels during a shot, the optimal length of a fluttering pattern $U = [u_1, \cdots, u_n]$ is n. As demonstrated in [24], if the object moves twice as fast, the effective PSF is stretched

$\frac{1}{2n}[u_1, u_1, \cdots, u_n, u_n]$ and the invertivility of the PSF cannot be guaranteed.

We show that complementary set of sequences minimizes the loss of spectral information even when the effective PSFs are super-sampled or stretched due to the velocity of an object. As an example, we derive the change of MTF due to a stretched sequence by a factor 2:

$$b_i = \sum_{j=0}^{2n-i-1} U_{2n}U_{2n}(j+i)$$

$$= \sum_{p=0}^{n-q-1} [U_{2n}(2p)U_{2n}(2p+2q)+U_{2n}(2p+1)U_{2n}(2p+2q+1)]$$

$$= \sum_{p=0}^{n-q-1} [U_n(p)U_n(p+q) + U_n(p)U_n(p+q)] = 2\Psi_k,$$

$$\text{where} \quad j = 2p \quad \text{and} \quad i = 2q. \quad (5)$$

The variance of MTF of the stretched PSF is constant times bigger than the PSF as follows:

$$\sum_{i=1}^{n-1} b_i = 4\sum_{k=1}^{n-1} {\Psi_k}^2 = 2\int_0^1 [|\mathcal{F}(U_n)|^2 - n]^2 d\theta. \quad (6)$$

As mentioned in Sec. 2.1, the optimal bound of $\frac{1}{2}\int_0^1[\mathcal{F}(U_n) - n]d\theta$ in the complementary set of sequences is theoretically zero. Thus, the optimal bound of the decimated PSF also become zero. In practice, because our set of sequences is close to the optimal bound, the proposed complementary set can handle the velocity dependency issue and it can be shown for the case of any factor. Our system's robustness to the object velocity is also demonstrated in the Experiments Section.

2.3. Varying Exposure Video vs. Coded Exposure Video

To compare our coded exposure video framework with the varying exposure video [2], we analyze the upper bound of MTFs for these two methods. The main criteria for the comparisons are the variance, the minimum, and the mean of MTF. As shown in [27, 25], the MTF of a binary sequence in coded exposure photography has a direct impact on the performance of image deblurring. The variance and the mean of MTF are related to deconvolution noise, and the peakiness of the spectrum has an ill effect on deblurring since it destroys the spatial frequencies in the blurred image.

The MTF of the varying exposure method [2] is the joint spectrum of different durations of rectangle functions in the time domain (Fig. 2(b)). The upper bound of the joint MTF X_{vary} of p varying exposures is derived as

$$|X_{vary}(\omega)| = \sum_{i=1}^{p} |\mathcal{F}(\Pi(l_i))| = \sum_{i=1}^{p} |\frac{\sin\frac{l_i}{2}\omega}{\sin\frac{\omega}{2}}| \leq |\frac{p}{\sin\frac{\omega}{2}}|, \quad (7)$$

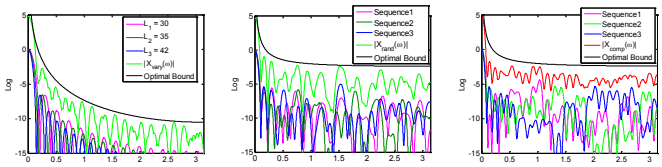

(a) Joint MTF of [2] (b) Joint MTF of [27] (c) Proposed

Figure 2. Joint MTF of each method and its theoretical upper bound. (a) Varying exposure video [2]. (b) Different fluttering patterns by random sample search [27]. (c) The proposed method by complementary set of fluttering patterns.

where $\Pi(l)$ denotes a rectangle function of length l, and ω is a circular frequency at $[-\pi, \pi]$.

To compute the upper bound for the coded exposure video, let Φ denote a binary sequence of $+1$'s and -1's. Parker *et al.* [26] showed that the sum of all the Fourier transform components of a complementary set of p sequences $\Phi_i, i = [1, \cdots, p]$ of length n is at most $\sqrt{pn}$. Since a fluttering pattern in the coded exposure imaging is made of $+1$'s and 0's due to its physical nature, the upper bound of the joint MTF X_{comp} of a complementary set is computed as

$$|X_{comp}(\omega)| = \frac{1}{2}\sum_{i=1}^{p} |\mathcal{F}(\Phi_i + \Pi(n))| \quad (8)$$

$$\leq \frac{1}{2}\sum_{i=1}^{p} |\mathcal{F}(\Phi_i)| + \frac{1}{2}\sum_{i=1}^{p} |\mathcal{F}(\Pi(n))| \leq \frac{1}{2}\sqrt{pn} + |\frac{p}{2\sin\frac{\omega}{2}}|.$$

Fig. 2 compares the joint MTF of the varying exposure video and the coded exposure video with the theoretical upper bound in Eq. (7) and Eq. (8). For the varying exposure video in (a), the exposure lengths of $[30, 35, 42]$ are used as in [2]. For the coded exposure video, we use three random sequences from [27] in (b) and our complementary set of binary sequences in (c) which will be explained in the next section. As can be seen in the figure, no null frequency is observed at the MTFs of each coded pattern in the complementary set. This means that each single frame becomes invertible as with the conventional coded exposure imaging [27, 14]. In (b), the peaky spectrums of the random binary sequences are moderated but the variance of the joint MTF is still large. The peaky spectrums of each sequence in the complementary set are well compensated by the joint MTF (c), and the joint MTF (c) has much flatter and higher MTF than the joint MTFs of both the varying exposure method (a) and the set of the random sample sequences (b).

Theoretical upper bounds as well as the actual performance measurements of the MTF properties for the varying exposure video and the coded exposure video are plotted in Fig. 3. To verify the effectiveness of the complementary set of fluttering patterns, the random sample search method in [27] is used to generate the binary sequences for single

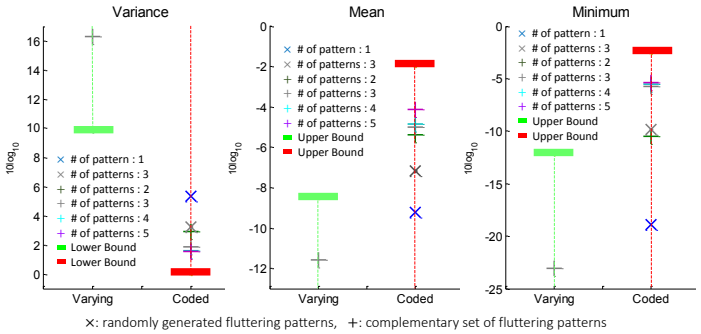

Figure 3. The theoretical upper bound and the actual performance measurement of the varying exposure video and the coded exposure video in terms of MTF properties.

image and three images cases. Although the MTFs of both the coded exposure and the varying exposure do not reach the lower (variance) and the upper bound (mean and minimum), the coded exposure patterns shows better MTF properties than both the varying exposure method and the set of random sequences. Specifically, the complementary set has a jointly flat spectrum with higher mean and minimum MTF value which are even better than the theoretical bounds of the varying exposure method. This shows that the complementary set preserves spatial frequencies well by compensating frequency losses in each frame. It is worth noting that while utilizing all the sequences in a complementary set is ideal in theory, utilizing a partial set of the complementary set is also effective as shown in Fig. 2 and Fig. 3.

3. Coded Exposure Video

3.1. Hardware Setup

Constructing a hardware system for the coded exposure video is not trivial. We implemented the coded exposure video system using a Point Grey Flea3 GigE camera which supports the multiple exposure pulse-width mode (Trigger Mode 5) and a ATmega128 micro-controller to generate external trigger pulses (Fig. 4). The micro-controller sends the binary sequence signal to the camera as external triggers through the serial communication (step 1 in Fig. 4). The camera finishes taking a photo after c number of peaks in the sequence (gray area in the figure), which indicates the end of a sequence (step 2). The camera then transmits the image and the signal to the computer (step 3) and the computer passes the parameter c of the next sequence to the camera (step 4). This process is repeated again to take a new set of images under a new sequence (step 1). We used this system to capture both the varying exposure video and the coded exposure video. Each shutter chop is 1ms long and the frame rate is fixed at 5 frames per second regardless of the sequence length due to the hardware limitation. The implementation manual and the source

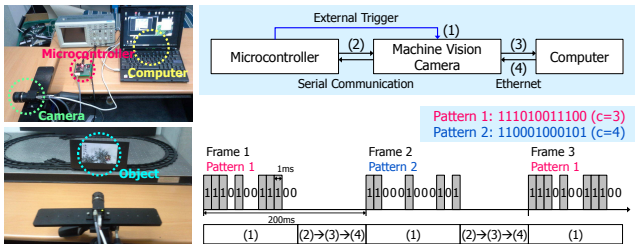

Figure 4. Hardware Setup for the Coded Exposure Video.

code of our framework are released in our website https://sites.google.com/site/hgjeoncv/complementary_sets.

3.2. Sequence Generation

In the coded exposure imaging, a fluttering pattern of a camera shutter generally consists of a sequence longer than 20 bits, or even longer than 100 bits. Since the length of the fluttering pattern may vary due to the illumination condition or the object motion, it is beneficial to have a flexibility in the length of the pattern. In this subsection, we introduce a method for generating a complementary set of fluttering patterns of flexible length.

Our strategy for obtaining the flexibility in the sequence length is to generate the complementary set by expanding a small-sized initial set that is known to be a complementary set. Since the research in the complementary set construction has a long history, many known complementary sets exist such as

$$\mathbf{\Delta} = \left[\begin{array}{cc} 0 & 1 \\ 0 & 0 \end{array}\right], \left[\begin{array}{c} 11101101 \\ 11100010 \end{array}\right], \left[\begin{array}{c} 000010100100 \\ 001001111101 \\ 101000100011 \\ 001110010111 \end{array}\right],$$

where $\mathbf{\Delta}$ denotes a complementary set in a matrix form. In $\mathbf{\Delta}$, each row vector represents one sequence and the set of all row vectors is a complementary set.

From an initial complementary set $\Delta_{(p,n)}$ which consists of p sequences of length n, we can iteratively generate larger complementary sets [38]. With a complementary set Δ, a new complementary set $\mathbf{\Delta}^1$ with larger length sequence is obtained by

$$\mathbf{\Delta}^1 = \left[\begin{array}{cccc} \mathbf{\Delta} & \mathbf{\Delta} & \bar{\mathbf{\Delta}} & \mathbf{\Delta} \\ \bar{\mathbf{\Delta}} & \mathbf{\Delta} & \mathbf{\Delta} & \mathbf{\Delta} \end{array}\right], \tag{9}$$

where $\bar{\mathbf{\Delta}}$ denotes the matrix with all the elements δs in $\mathbf{\Delta}$ flipped. After applying the expansion t times, we obtain a complementary matrix $\Delta^t \in \mathbb{R}^{2^t p \times 4^t n}$, which contains $2^t p$ sequences of length $4^t n$.

Another option for generating variable length sequences is to divide $\mathbf{\Delta}$ into two matrices with the same length as

$$\mathbf{\Delta} = \left[\begin{array}{cc} \mathbf{\Delta}_L & \mathbf{\Delta}_R \end{array}\right]. \tag{10}$$

In this case, both matrices $\mathbf{\Delta}_L$ and $\mathbf{\Delta}_R$ become complementary sets [10].

With the two matrix operations in Eq. (9) and Eq. (10), we can generate a complementary set, whose size is $2^t p \times 2^{2t} n$ or $2^t p \times 2^{2t-1} n$. Since there are many well-known initial complementary sets with various sizes, we can generate complementary sets with huge flexibility of sequence length using the two methods.

In the video deblurring scenario, the required number of sequences (or images) are usually limited to 2∼5 because it is enough to compensate for the frequency losses and taking many pictures may create additional problems such as the alignment and the field-of-view issue. Therefore, we first generate a complementary set that fits with the required sequence length, and then select the required number of sequences among many candidate sequences in the set.

As for the criteria for selecting sequences from the available set of sequences, we consider the number of open chops. In general, the generated sequences have similar number of open chops, e.g. $n/2$, however it could be slightly different especially for short length sequences. In this case, selecting sequences with equal number of open chops can be an important criterion to avoid flickering between frames.

3.3. A Blurred Object Extraction and Deblurring

One practical issue with the coded exposure imaging is to extract an accurate matte image for the moving object deblurring. It is challenging because a blur profile becomes locally non-smooth due to the exposure fluttering. Agrawal and Xu [1] proposed the fluttering pattern design rules that minimize the transitions and maximize continuous open chops, and showed that both criteria of PSF estimation [8] and invertibility can be achieved. In [36], a blurred object is extracted from a static background with user strokes in order to estimate motion paths and magnitudes. McCloskey *et al*. [25] presented a PSF estimation algorithm for coded exposure assuming that the image only contains a motion blurred object. In this paper, we deal with this matting issue by jointly estimating the PSF, object matting, and the multi-image deblurring. We assume that the images are captured from a static camera and a moving object is blurred by a constant velocity 1-D motion.

Initialization To accurately extract the blurred object (Fig. 5(a)), we first capture background images and model each pixel of the background using a Gaussian mixture model (GMM). When an object passes over the background, we estimate an initial foreground layer by computing the Mahalanobis distance between pixels of each image and the background model. Since the estimated layers are somewhat noisy, we refine the layers by applying morphological operations and make trimaps. Using the trimaps (Fig. 5(b)), we extract the blurred object at each image via the closed form matting [18].

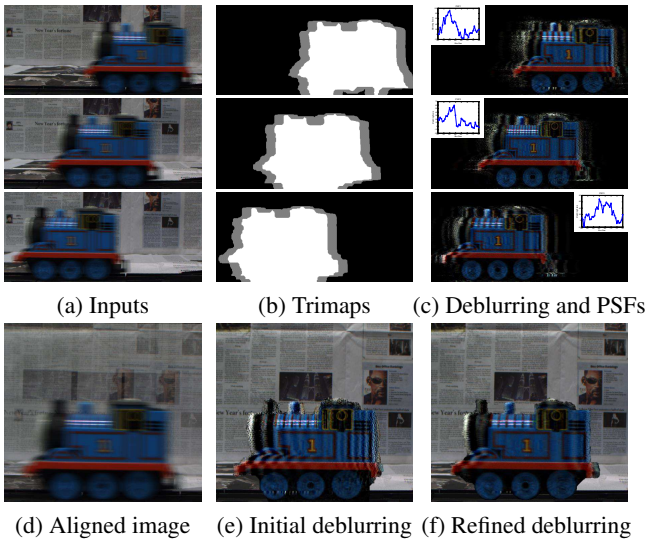

(a) Inputs (b) Trimaps (c) Deblurring and PSFs

(d) Aligned image (e) Initial deblurring (f) Refined deblurring

Figure 5. Multi-image Deblurring Procedure

After the object matting, we estimate the PSF of each image based on the method in [25], which can handle the cases of constant velocity, constant acceleration, and harmonic motion. Specifically, we first perform the radon transform and choose the direction with the maximal variance as a blur direction. This is because high spatial frequencies of a blurred image is collapsed according to a blur direction. Then, we compute matching scores between the power spectral density of the blurred image and the MTF of the fluttering pattern for various blur size. We determine the size of blur by choosing the highest matching score. With this method, we estimate the blur kernel of each coded blurred image independently (Fig. 5(c)). This is useful because we do not suffer from the violation of the constant motion assumption between frames that often occurs in practice.

With the estimated PSFs, the captured images are deblurred independently. Then, we align all images by affine matrix of the deblurred images using SIFT feature matching [22], and merge all the captured images along with the alpha maps (Fig. 5(d)).

Iterative Refinement After the initialization, we iteratively optimize between a latent image and the segmentation masks. Based on the merged image with the PSFs, we perform a non-blind multi-image deblurring by minimizing the following energy term:

$$\underset{Y}{\operatorname{argmin}} \sum_{j=1}^{m} \|B_j - K_j Y\|^2 + \lambda_d \|\nabla Y\|^\rho, \qquad (11)$$

where Y is a latent deblurred image, ∇Y is the gradient of the latent image, B_j is a set of linearly blurred images captured by a set of PSF matrices K_j. λ_d is the smoothness

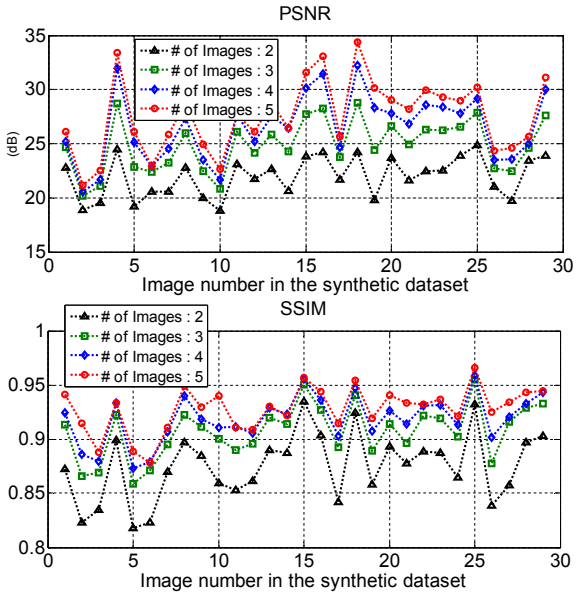

Figure 6. The performance variations of the proposed method according to the number of fluttering patterns used.

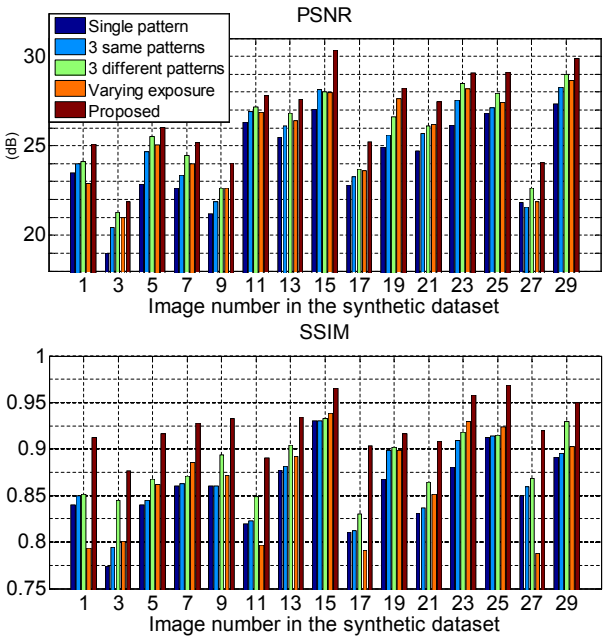

Figure 7. The quantitative comparisons of different methods on image deblurring.

weight and m is the number of images. We set $\rho = 0.8$ for image deblurring [17] and $\rho = 0.5$ for the merged alpha map deblurring $\overline{\alpha}$ according to [36]. The deblurred alpha map $\overline{\alpha}$ is re-blurred to obtain a guidance alpha map $\widehat{\alpha}$ which is incorporated as a soft constraint in the close form matting to refine the alpha map α for the moving object [16]:

$$\underset{\alpha}{\operatorname{argmin}}\, \alpha^T \mathbf{L}\alpha + \lambda_m(\alpha - \widehat{\alpha})^T \mathbf{D}(\alpha - \widehat{\alpha}), \qquad (12)$$

where $\mathbf{L}$ is the Laplacian matrix of the closed form matting, $\mathbf{D}$ is a diagonal matrix and λ_m is the weight for the soft constraint.

With the refined alpha maps, we optimize the set of affine matrices $\mathbf{H}$ that minimizes the energy function similar to the stereo matching as follows:

$$\underset{\mathbf{H}}{\operatorname{argmin}} \sum_{j=1}^{m-1} \{\lambda_a \min(|X_{ref} - H_j X_j|, \tau_{color}) + (1-\lambda_a)\min(|\nabla X_{ref} - \nabla(H_j X_j)|, \tau_{grad})\},$$

where X is independently deblurred image and X_{ref} is the reference view. λ_a balances the color and the gradient terms, and $\tau_{color}, \tau_{grad}$ are truncation values to account for outliers correspondences.

As shown in Fig. 5(f), our algorithm shows a promising result of moving object deblurring in complex background. The refinement is iterated 2 or 3 times for the final result and takes 5 minutes for an image with 800×600 resolution in our MATLAB implementation. We empirically set $\{\lambda_d, \lambda_m, \lambda_a, \tau_{color}, \tau_{grad}\} = \{0.01, 0.1, 0.5, 0.3, 0.5\}$.

4. Experiments

To verify the effectiveness of the proposed method, we perform both quantitative and qualitative comparisons with other computational imaging methods; the coded exposure imaging [27] and the varying exposure video [2]. For the coded exposure method [27], we use a fluttering pattern of length 48 generated by the author's code[1]. The exposure sequences $[30, 35, 42ms]$ stated in [2] is used for the varying exposure method. The fluttering patterns of length 48 of the proposed method is generated by applying Eq. (9) once to the initial set [2].

4.1. Synthetic Experiments

For quantitative evaluations, we perform synthetic experiments. As the synthetic data, we use 29 images downloaded from Kodak Lossless True Color Image Suite [30]. Image blur is simulated by the 1D filtering with different exposure sequences generated by each method. To simulate a real photography, we add the intensity dependent Gaussian noise with the standard deviation $\sigma = 0.01\sqrt{i}$ where i is the noise-free intensity of the blurred images in $[0, 1]$ [31]. The peak signal-to-noise ratio (PSNR) and the gray-scale structural similarity (SSIM) [41] are used as the quality metrics. For fair comparisons, we conduct parameter sweeps for image deblurring and the highest PSNR and SSIM values of each image/method are reported.

[1] www.umiacs.umd.edu/~aagrawal/MotionBlur/SearchBestSeq.zip

[2] The initial set we used in this work is [000010100100; 001001111101; 101000100011; 001110010111]

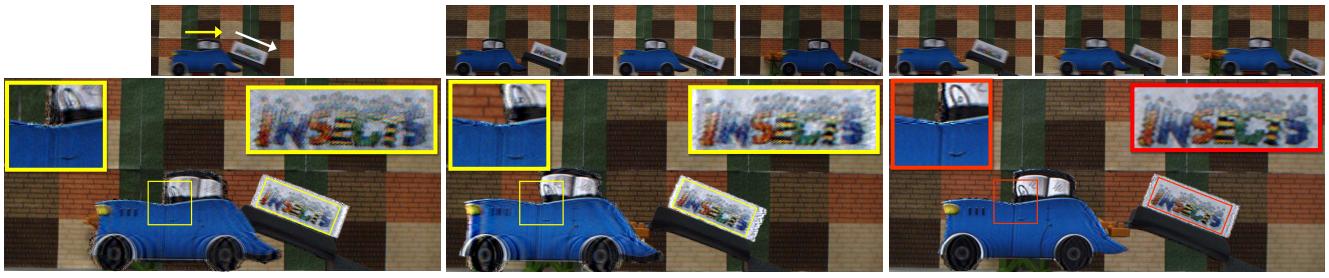

(a) Coded Exposure [27] (b) Varying Exposure [2] (c) Proposed

Figure 9. Multiple objects deblurring with different velocities and directions. Blur size of the car (close) and the panel (far) (unit: pixel): (a) 50 and 45. (b) [36 44 39] and [25 31 27]. (c) [46 50 52] and [35 38 44].

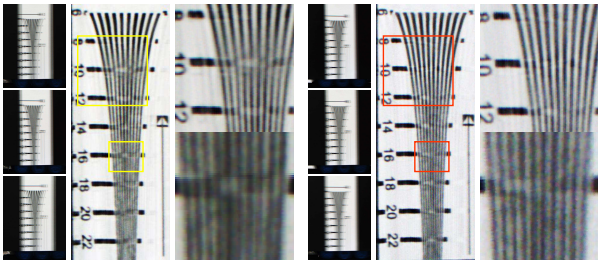

(a) A random sequences set (b) Proposed

Figure 8. Comparison of results using a random set and the proposed complementary set when PSFs are stretched (Blur size : 96 pixels).

Fig. 6 reports the averaged PSNR and SSIM of the proposed method according to the number of images used. We can observe that better performance is achieved with more images, however the performance gain ratio is reduced as the number of images increases. The experiment shows that utilizing three fluttering patterns is a good trade-off between the performance gain and the burden of multi-image deblurring for the proposed method. Therefore we use three fluttering patterns for the remaining experiments.

Quantitative comparisons of different methods are shown in Fig. 7[3]. For a complete verification, we additionally consider two sets of coded exposure sequences generated by the random sample search [27]. Each set of three sequences consists of the same fluttering pattern and three different patterns, respectively. We include the two set of sequences as baseline extensions of a single coded exposure to coded exposure video. The proposed method outperforms the previous methods for all the dataset, with large margins especially in SSIM. This is because the proposed method yields high-quality deblurring results while the previous methods fail to recover textured regions due to the loss of high spatial frequencies. Fig. 1 shows examples of the synthetic result. As shown in the figures, our method outperforms the other methods both qualitatively and quantitatively.

[3]Here, we only report odd numbered dataset results due to limited page space. All PSNR and SSIM values are reported in supplementary material.

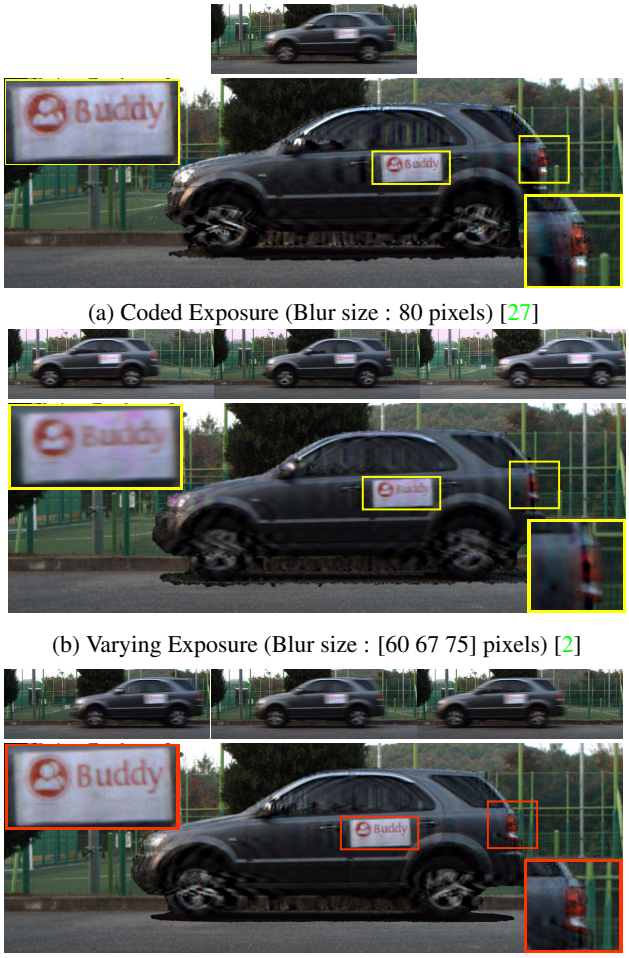

(a) Coded Exposure (Blur size : 80 pixels) [27]

(b) Varying Exposure (Blur size : [60 67 75] pixels) [2]

(c) Proposed (Blur size : [80 80 82] pixels)

Figure 10. Outdoor Experiment

4.2. Real-world Experiments

In Fig. 8, we show an empirical validation of the performance issue discussed in Sec. 2.2. We captured a resolution chart in a carefully controlled environment, and the chart moved two pixels during one exposure chop. We compare our complementary set with a set of randomly gener-

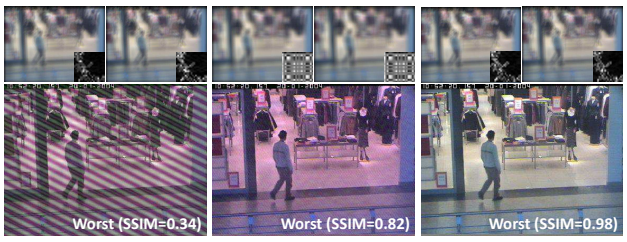

(a) Random sets (b) MURA (c) Proposed

Figure 11. Privacy-protecting video surveillance

ated fluttering patterns. As shown in Fig. 8, when PSF is stretched, the deblurred image captured by the random sequence set has noticeable artifacts around edges. On the other hand, the proposed complementary set preserves details on the resolution chart well.

Fig. 9 shows the results of deblurring multiple objects with different velocities. To segment each object trimap separately, we performed multi-label optimization via graph-cuts [3]. Then, each object was deblurred and pasted onto the background independently. In Fig. 9, one object is highly textured and moving fast, while the other one is lowly textured and moving slow. The proposed method shows the best results compared to other deblurring methods.

We then performed another real-world experiment in outdoor by capturing a fast moving object as shown in Fig. 10. The motion direction and the blur kernel is estimated automatically in the complex background that has similar color as the moving car. Once again, our coded exposure video scheme outperforms the other two methods.

4.3. Application to a privacy protection method for video surveillance

The privacy protection for video surveillance has become an important issue recently as the video surveillance has become a commonplace. Various attempts have been made to address the issue in computer vision [40, 5] and an interesting study is the use of a coprime blur scheme, which strategically blurs surveillance videos for privacy protection [19].

The coprime blur scheme encrypts video streams by applying two different blur kernels which satisfy *coprimality*, and forms a public stream and a private stream. An unblurred stream can be recovered by a coprime deblurring algorithm when both the private and public streams can be accessed. Since it is very difficult to apply blind deconvolution with only a public stream, the privacy in video streams is protected and higher level of security can be achieved by choosing different blur kernels for each frame. In [19], Li *et al*. synthesized the coprime blur kernels from two binary sequences and presented an efficient deblurring algorithm. They also highlighted the importance of constructing a bank of blur kernels with flat spectrum because it directly affects the security-level and the quality of recovered videos.

Our complementary sets of fluttering patterns can be directly applied to design the coprime blur kernels in the same manner[4]. Because we can generate diverse sets of fluttering patterns with various lengths and flat spectrum, our method is suitable to achieve both high-level security and high-quality recovery.

We performed an experiment to show the effectiveness of our framework applied to the coprime blur scheme. We first generate a pair of coprime blur kernel by using the modified uniformly redundant array (MURA) [11], and six pairs of coprime blur kernels by using the random sample search [27] and our complementary sequences. Then, we encrypt the video[5] by synthetically blurring each frame and decrypt it according to the coprime method in [19][6].

Both the encryption and the decryption results by the coprime method are shown in Fig. 11. The first rows represent encrypted frames with coprime blur kernels and the second rows show the deblurred results. The coprime method consistently produces high quality reconstruction results with our complementary sequences while it suffers from severe artifacts in some cases when other sequences are used[7]. This is because the random sample search fails to generate good sequences with long length due to the large search space as discussed in [14] and the MURA includes deep dips that result in spectral leakage as shown in [27]. On the other hand, our complementary sequences are able to produce good sequence pairs with various length and sets.

5. Conclusion

In this paper, we introduced a novel coded exposure video framework for multi-image deblurring. The proposed method essentially combines the coded exposure imaging and the varying exposure video, taking advantages of the two methods to yield superior deblurring results. The limitation of the current work is that we only solve for 1D linear blur of a constant velocity object. Note that many real world object motions such as a walking person or a moving car result in 1D motion blur as mentioned in [27]. In addition, affine blur from slanted blurred scene can be interpreted as a 1D motion blur problem [27]. In the future, we would like to extend our method to overcome the current limitations such as known background and linear motion assumptions as well as to apply our framework for multi-image super-resolution and visual odometry for robotics.

[4] According to [15], two different sequences are generally coprime. To verify the coprimality of complementary pairs of sequences, we generated 120 complementary pairs of sequences of length 256 and confirmed that all the pairs satisfy the coprimality by the Euclid's algorithm [9].

[5] dataset: http://homepages.inf.ed.ac.uk/rbf/CAVIAR/

[6] We used the deblurring code by the author to decrypt the video - http://fengl.org/publications/

[7] The corresponding video is available on supplementary material.

Acknowledgements. This work was supported by the National Research Foundation of Korea(NRF) grant funded by the Korea government(MSIP) (No.2010- 0028680). Hae-Gon Jeon was partially supported by Global PH.D Fellowship Program through the National Research Foundation of Korea(NRF) funded by the Ministry of Education (NRF-2015H1A2A1034617).

References

[1] A. Agrawal and Y. Xu. Coded exposure deblurring: Optimized codes for PSF estimation and invertibility. In *Proceedings of IEEE Conference on Computer Vision and Pattern Recognition (CVPR)*, 2009.

[2] A. Agrawal, Y. Xu, and R. Raskar. Invertible motion blur in video. In *Proceedings of ACM SIGGRAPH*, 2009.

[3] Y. Boykov, O. Veksler, and R. Zabih. Fast approximate energy minimization via graph cuts. *IEEE Transactions on Pattern Analysis and Machine Intelligence (PAMI)*, 23(11):1222–1239, 2001.

[4] J.-F. Cai, H. Ji, C. Liu, and Z. Shen. Blind motion deblurring using multiple images. *Journal of Computational Physics*, 228(14):5057–5071, 2009.

[5] A. Chattopadhyay and T. E. Boult. Privacycam: a privacy preserving camera using uclinux on the blackfin dsp. In *Proceedings of IEEE Conference on Computer Vision and Pattern Recognition (CVPR)*, 2007.

[6] J. Chen, L. Yuan, C. keung Tang, and L. Quan. Robust dual motion deblurring. In *Proceedings of IEEE Conference on Computer Vision and Pattern Recognition (CVPR)*, 2008.

[7] S. Cho, J. Wang, and S. Lee. Video deblurring for hand-held cameras using patch-based synthesis. *ACM Transactions on Graphics*, 31(4):64:1–64:9, 2012.

[8] S. Dai and Y. Wu. Motion from blur. In *Proceedings of IEEE Conference on Computer Vision and Pattern Recognition (CVPR)*, 2008.

[9] E. K. Donald. The art of computer programming. *Sorting and searching*, 3:426–458, 1999.

[10] P. Fan, N. Suehiro, N. Kuroyanagi, and X. Deng. Class of binary sequences with zero correlation zone. In *Electronics Letters*, volume 35, pages 777–779, 1999.

[11] S. R. Gottesman and E. Fenimore. New family of binary arrays for coded aperture imaging. *Applied optics*, 28(20):4344–4352, 1989.

[12] J. Holloway, A. C. Sankaranarayanan, A. Veeraraghavan, and S. Tambe. Flutter shutter video camera for compressive sensing of videos. In *Proceedings of IEEE International Conference on Computational Photography (ICCP)*, 2012.

[13] J. M. Jensen, H. E. Jensen, and T. Høholdt. The merit factor of binary sequences related to difference sets. *IEEE Transactions on Information Theory*, 37(3):617–626, 1991.

[14] H.-G. Jeon, J.-Y. Lee, Y. Han, S. J. Kim, and I. S. Kweon. Fluttering pattern generation using modified Legendre sequence for coded exposure imaging. In *Proceedings of IEEE International Conference on Computer Vision (ICCV)*, 2013.

[15] E. Kaltofen, Z. Yang, and L. Zhi. On probabilistic analysis of randomization in hybrid symbolic-numeric algorithms. In *Proceedings of the international workshop on Symbolic-numeric computation*, 2007.

[16] S. Kim, Y.-W. Tai, Y. Bok, H. Kim, and I. S. Kweon. Two-phase approach for multi-view object extraction. In *Proceedings of International Conference on Image Processing (ICIP)*, 2011.

[17] A. Levin, R. Fergus, F. Durand, and W. T. Freeman. Image and depth from a conventional camera with a coded aperture. *ACM Transactions on Graphics*, 26(3), 2007.

[18] A. Levin, D. Lischinski, and Y. Weiss. A closed-form solution to natural image matting. *IEEE Transactions on Pattern Analysis and Machine Intelligence (PAMI)*, 30(2):228–242, 2008.

[19] F. Li, Z. Li, D. Saunders, and J. Yu. A theory of coprime blurred pairs. In *Proceedings of IEEE International Conference on Computer Vision (ICCV)*, 2011.

[20] D. Liu, J. Gu, Y. Hitomi, M. Gupta, T. Mitsunaga, and S. Nayar. Efficient space-time sampling with pixel-wise coded exposure for high speed imaging. *IEEE Transactions on Pattern Analysis and Machine Intelligence (PAMI)*, 99:1, 2013.

[21] P. Llull, X. Liao, X. Yuan, J. Yang, D. Kittle, L. Carin, G. Sapiro, and D. J. Brady. Coded aperture compressive temporal imaging. *Optics express*, 21(9):10526–10545, 2013.

[22] D. G. Lowe. Distinctive image features from scale-invariant keypoints. *International Journal on Computer Vision (IJCV)*, 60(2):91–110, 2004.

[23] L. B. Lucy. An iterative technique for the rectification of observed distributions. *Astronomical Journal*, 79:745–754, 1974.

[24] S. McCloskey. Velocity-dependent shutter sequences for motion deblurring. In *Proceedings of European Conference on Computer Vision (ECCV)*, pages 309–322, 2010.

[25] S. McCloskey, Y. Ding, and J. Yu. Design and estimation of coded exposure point spread functions. *IEEE Transactions on Pattern Analysis and Machine Intelligence (PAMI)*, 34(10):2071–2077, 2012.

[26] M. G. Parker, K. G. Paterson, and C. Tellambura. *Golay Complementary Sequences*. In Wiley Encyclopedia of Telecommunications, 2003.

[27] R. Raskar, A. Agrawal, and J. Tumblin. Coded exposure photography: motion deblurring using fluttered shutter. *ACM Transactions on Graphics*, 25(3):795–804, 2006.

[28] D. Reddy, A. Veeraraghavan, and R. Chellappa. P2C2: Programmable pixel compressive camera for high speed imaging. In *Proceedings of IEEE Conference on Computer Vision and Pattern Recognition (CVPR)*, pages 329–336.

[29] W. H. Richardson. Bayesian-based iterative method of image restoration. *Journal of the Optical Society of America*, 62:55–59, 1972.

[30] R.W.Franzen. Kodak lossless true color image suite, June 1999.

[31] Y. Y. Schechner, S. K. Nayar, and P. N. Belhumeur. Multiplexing for optimal lighting. *IEEE Transactions on Pattern Analysis and Machine Intelligence (PAMI)*, 29(8):1339–1354, Aug 2007.

[32] O. Shahar, A. Faktor, and M. Irani. Space-time super-resolution from a single video. In *Proceedings of IEEE Conference on Computer Vision and Pattern Recognition (CVPR)*, 2011.

[33] E. Shechtman, Y. Caspi, and M. Irani. Space-time super-resolution. *IEEE Transactions on Pattern Analysis and Machine Intelligence (PAMI)*, 27(4):531–545, 2005.

[34] M. Soltanalian, M. M. Naghsh, and P. Stoica. A fast algorithm for designing complementary sets of sequences. *Signal Processing*, 93(7):2096–2102, 2013.

[35] P. Spasojevic and C. N. Georghiades. Complementary sequences for ISI channel estimation. *IEEE Transactions on Information Theory*, 47(3):1145–1152, 2001.

[36] Y.-W. Tai, N. Kong, S. Lin, and S. Y. Shin. Coded exposure imaging for projective motion deblurring. In *Proceedings of IEEE Conference on Computer Vision and Pattern Recognition (CVPR)*, 2010.

[37] Y. Tendero, J.-M. Morel, and B. Rougé. The flutter shutter paradox. *SIAM Journal on Imaging Sciences*, 6(2):813–847, 2013.

[38] C.-C. Tseng and C. L. Liu. Complementary sets of sequences. *IEEE Transactions on Information Theory*, 18(5):644–652, 1972.

[39] A. Ukil. Low autocorrelation binary sequences: Number theory-based analysis for minimum energy level, barker codes. *Digital Signal Processing*, 20(2):483–495, 2010.

[40] M. Upmanyu, A. M. Namboodiri, K. Srinathan, and C. Jawahar. Efficient privacy preserving video surveillance. In *Proceedings of IEEE International Conference on Computer Vision (ICCV)*, 2009.

[41] Z. Wang, A. C. Bovik, H. R. Sheikh, and E. P. Simoncelli. Image quality assessment: from error visibility to structural similarity. *IEEE Transactions on Image Processing (TIP)*, 13(4):600–612, 2004.

[42] N. Wiener. *Extrapolation, Interpolation, and Smoothing of Stationary Time Series*. The MIT Press, 1964.

[43] L. Yuan, J. Sun, L. Quan, and H.-Y. Shum. Image deblurring with blurred/noisy image pairs. *ACM Transactions on Graphics*, 26(3), 2007.